Please cite this article in press as: Xue et al., Phenylpropanoid Derivatives Are Essential Components of Sporopollenin in Vascular Plants, Molecular Plant (2020), https://doi.org/10.1016/j.molp.2020.08.005

Molecular Plant
Research Report

CellPress
Partner Journal

Phenylpropanoid Derivatives Are Essential Components of Sporopollenin in Vascular Plants

Jing-Shi Xue[1,7], Baocai Zhang[3,7], HuaDong Zhan[4,7], Yong-Lin Lv[1], Xin-Lei Jia[1], TianHua Wang[1], Nai-Ying Yang[1], Yu-Xia Lou[1], Zai-Bao Zhang[5], Wen-Jing Hu[1], Jinshan Gui[2], Jianguo Cao[1], Ping Xu[1], Yihua Zhou[3], Jin-Feng Hu[6], Laigeng Li[2,*] and Zhong-Nan Yang[1,*]

[1]Shanghai Key Laboratory of Plant Molecular Sciences, College of Life Sciences, Shanghai Normal University, Shanghai 200234, China

[2]National Key Laboratory of Plant Molecular Genetics & CAS Center for Excellence in Molecular Plant Sciences, Institute of Plant Physiology and Ecology, Chinese Academy of Sciences, Beijing 200032, China

[3]State Key Laboratory of Plant Genomics, Institute of Genetics and Developmental Biology, Chinese Academy of Sciences, Beijing 100101, China

[4]State Key Laboratory of Crop Genetics and Germplasm Enhancement, College of Agriculture, Nanjing Agricultural University, Nanjing 210095, China

[5]College of Life Science, Xinyang Normal University, Xinyang, Henan 464000, China

[6]Department of Natural Products Chemistry, School of Pharmacy, Fudan University, No. 826 Zhangheng Road, Shanghai, 201203, China

[7]These authors contributed equally to this article.

***Correspondence: Laigeng Li (lgli@sibs.ac.cn), Zhong-Nan Yang (znyang@shnu.edu.cn)**

https://doi.org/10.1016/j.molp.2020.08.005

ABSTRACT

The outer wall of pollen and spores, namely the exine, is composed of sporopollenin, which is highly resistant to chemical reagents and enzymes. In this study, we demonstrated that phenylpropanoid pathway derivatives are essential components of sporopollenin in seed plants. Spectral analyses showed that the autofluorescence of *Lilium* and *Arabidopsis* sporopollenin is similar to that of lignin. Thioacidolysis and NMR analyses of pollen from *Lilium* and *Cryptomeria* further revealed that the sporopollenin of seed plants contains phenylpropanoid derivatives, including *p*-hydroxybenzoate (*p*-BA), *p*-coumarate (*p*-CA), ferulate (FA), and lignin guaiacyl (G) units. The phenylpropanoid pathway is expressed in the tapetum in *Arabidopsis*, consistent with the fact that the sporopollenin precursor originates from the tapetum. Further germination and comet assays showed that this pathway plays an important role in protection of pollen against UV radiation. In the pteridophyte plant species *Ophioglossum vulgatum* and *Lycopodium clavata*, phenylpropanoid derivatives including *p*-BA and *p*-CA were also detected, but G units were not. Taken together, our results indicate that phenylpropanoid derivatives are essential for sporopollenin synthesis in vascular plants. In addition, sporopollenin autofluorescence spectra of bryophytes, such as *Physcomitrella* and *Haplocladium*, exhibit distinct characteristics compared with those of vascular plants, indicating the diversity of sporopollenin among land plants.

Key words: sporopollenin, pollen cell wall, phenylpropanoid pathway

Xue J.-S., Zhang B., Zhan H., Lv Y.-L., Jia X.-L., Wang T., Yang N.-Y., Lou Y.-X., Zhang Z.-B., Hu W.-J., Gui J., Cao J., Xu P., Zhou Y., Hu J.-F., Li L., and Yang Z.-N. (2020). Phenylpropanoid Derivatives Are Essential Components of Sporopollenin in Vascular Plants. Mol. Plant. **13**, 1–10.

INTRODUCTION

The pollen cell wall is a conserved structure that effectively protects male gametes from environmental stresses (Wellman, 2004). The pollen cell wall is divided into exine and intine. The exine is highly resistant to chemical reagents and enzymes. The term sporopollenin describes the entire resistant material of exine (Brooks and Shaw, 1978; Ariizumi and Toriyama, 2010; Quilichini et al., 2015; Li et al., 2019). However, because the composition of sporopollenin is not fully understood, the mechanism underlying its protective qualities remains elusive (Quilichini et al., 2015).

Attempts to understand sporopollenin composition at the molecular level have a long history (Holt and Bennett, 2014). Biochemical evidence suggests that sporopollenin contains aliphatic units (Guilford et al., 1988; Domínguez et al., 1999; Bubert et al., 2002; Quilichini et al., 2015; Li et al., 2019). In *Arabidopsis thaliana* and *Oryza sativa*, disruption of genes encoding aliphatic unit modifying enzymes results in defective sporopollenin (Aarts et al., 1997; Ariizumi and Toriyama, 2010; de Azevedo Souza et

Published by the Molecular Plant Shanghai Editorial Office in association with Cell Press, an imprint of Elsevier Inc., on behalf of CSPB and IPPE, CAS.

Please cite this article in press as: Xue et al., Phenylpropanoid Derivatives Are Essential Components of Sporopollenin in Vascular Plants, Molecular Plant (2020), https://doi.org/10.1016/j.molp.2020.08.005

al., 2009; Dobritsa et al., 2010; Dobritsa et al., 2009; Grienenberger et al., 2010; Kim et al., 2010; Li et al., 2010; Morant and Bak, 2007; Quilichini et al., 2015; Shi et al., 2011). Other components, such as carotenoids (Brooks and Shaw, 1968) and silicon (Crang and May, 1974), have also been reported to be present in sporopollenin, but there are disagreements about this phenomenon (Prahl et al., 1986; Kawase and Takahashi, 1995). Using pyrolysis gas chromatography-mass spectrometry and the high-energy ball-milling-coupled thioacidolysis method, researchers detected several phenolic compounds, such as *p*-coumaric acid, ferulic acid, *p*-hydroxybenzaldehyde, and vanillic acid, in sporopollenin (Osthoff and Wiermann, 1987; Li et al., 2019). This discovery conflicts with the results from analyses using Fourier transform infrared spectroscopy and high-resolution X-ray photoelectron spectroscopy (Domínguez et al., 1999; Mikhael et al., 2020). Furthermore, cytological and genetic evidence indicating the requirement of phenolic compounds for sporopollenin formation is lacking. Thus, whether phenolic compounds are components of sporopollenin remains unclear.

The phenylpropanoid pathway provides intermediates for the synthesis of lignin, flavonoids, and hydroxycinnamoyl esters (Vogt, 2010). In this pathway, phenylalanine ammonia-lyase transfers phenylamine to cinnamic acid (Huang et al., 2010), which is further converted to *p*-coumaric acid by CINNAMATE-4-HYDROXYLASE (C4H) in *Arabidopsis* (Schilmiller et al., 2009). 4-COUMARATE:COA LIGASE (4CL) generates hydroxycinnamoyl-CoA from *p*-coumaric acids (Li et al., 2015). The lignin-specific biosynthetic pathway then uses hydroxycinnamoyl-CoA to produce monolignols. CINNAMOYL COA REDUCTASE (CCR) converts hydroxycinnamoyl-CoA into hydroxycinnamyl aldehyde, which is further reduced to hydroxycinnamyl alcohol (monolignol) by CINNAMYL ALCOHOL DEHYDROGENASE (CAD) (Boerjan et al., 2003). Several mutants of this pathway in *Arabidopsis* show defective lignin synthesis and are infertile, including the *c4h* single mutant, the *pal1 pal2 pal3 pal4* quadruple mutant, the *4cl1 4cl2 4cl3* triple mutant (Schilmiller et al., 2009; Huang et al., 2010; Li et al., 2015), and *ccr1* mutants (Derikvand et al., 2008).

In this study, we found that pollen wall fluorescence was similar to that of lignin in the xylem cell wall. To investigate the nature of pollen wall components emitting fluorescence similar to that of lignin, we performed a series of biochemical, genetic, and cytological analyses and found that the phenylpropanoid pathway was required for the synthesis of both lignin and sporopollenin in vascular plants. To dissect the composition of sporopollenin, we further studied the spectral and biochemical characteristics of sporopollenin in seed plants, pteridophytes, and bryophytes, and discovered that the characteristics of sporopollenin are distinct among the tested land plants.

RESULTS AND DISCUSSION

Lilium Sporopollenin Contains Derivatives from the Phenylpropanoid Pathway

It has been reported that the exine of pollen and spores is autofluorescent (Dobritsa et al., 2011; Mitsumoto et al., 2009; O'Connor et al., 2011; Willemse, 1972). We measured exine autofluorescence spectra in *Lilium brownii* and *Arabidopsis thaliana* in detail using excitation at 405 nm and recording the emission spectra from 420 to 700 nm (Figure 1A and 1B). In plants, lignin in the xylem cell wall also autofluoresces under UV light. Therefore, we examined the lignin spectrum under the same detection conditions and used chlorophyll as a control. The results showed that the fluorescence properties of lignin from the xylem and exine of the pollen wall were similar (Figure 1A and 1B). The main building blocks of lignin are monolignols (hydroxycinnamoyl alcohols), including coniferyl alcohol, sinapyl alcohol, and *p*-coumaryl alcohol, which are incorporated into lignin as guaiacyl (G), syringyl (S), and *p*-hydroxyphenyl (H) units, respectively (Boerjan et al., 2003). In addition to these units, several hydroxycinnamates, such as *p*-hydroxybenzoate (*p*-BA), *p*-coumarate (*p*-CA), and ferulate (FA), have been detected in xylem cell walls (Hatfield et al., 2016). To determine whether the pollen wall also contains lignin units, we collected pollen grains from *Lilium* and purified pollen walls using ethanol, chloroform/methanol, and acetone sequentially (see Methods) (Foster et al., 2010). After the treatment, the exine structure appeared unchanged (Figure 1C). To investigate its composition, the pollen wall was isolated and subjected to thioacidolysis, a classical method for lignin composition analysis (Lin and Dence, 1992). The resulting lysate was dissolved in deuterated dimethyl sulfoxide and subjected to 2D-NMR analysis. We consequently found that the lysate aromatic signals in heteronuclear single quantum coherence (HSQC) NMR spectra were identical to the C-H signals of the G unit and of the phenylpropanoid derivatives (*p*-BA, *p*-CA, and FA) (Figure 1D) shown in previously characterized cell wall lignin spectra (Karlen et al., 2018). These results suggest the presence of varied amounts of lignin G unit, *p*-BA, *p*-CA, and FA in sporopollenin, which was further corroborated by the cross peaks detected in total correlation spectroscopy of pollen wall lysate (Supplemental Figure 1). The G unit, *p*-BA, *p*-CA, and FA are known to be derived from the phenylpropanoid pathway. Hence, we conclude that phenylpropanoid derivatives are present in the pollen walls.

The Phenylpropanoid Pathway Is Expressed in the Tapetum

In *Arabidopsis*, several genes of the phenylpropanoid pathway have been identified (Bonawitz and Chapple, 2010; Xu et al., 2009), including *PAL1*, *C4H*, *4CL3*, *CCR1*, CAFFEOYL CoA-*O*-METHYLTRANSFERASE (*CCoAOMT*), CAFFEIC ACID *O*-METHYLTRANSFERASE (*COMT*), FERULIC ACID 5-HYDROXYLASE 1 (*F5H*), *CAD4*, and *CAD5* (Chang et al., 2011; Huang et al., 2010; Li et al., 2015; Schilmiller et al., 2009; Sibout et al., 2005; Thevenin et al., 2011). We fused the native promoter and coding regions of these genes to a fluorescent protein gene and constructed vectors to monitor their expression in plants. The constructs were individually introduced into *Arabidopsis* for transgenic expression. It is known that sporopollenin precursors are produced in the tapetum, which is a nutritive cell layer surrounding developing pollen grains, and further secreted into the anther locules from anther stage 7 (the tetrad stage) until degradation of the tapetum (Heslop-Harrison, 1962; Piffanelli et al., 1998; Sanders et al., 1999). The expression of the *PAL1*, *C4H*, *4CL3*, *CCR1*, *CCoAOMT*, *CAD4*, and *CAD5* genes was detected in the tapetum at all of these stages (Figure 2A and Supplemental

Please cite this article in press as: Xue et al., Phenylpropanoid Derivatives Are Essential Components of Sporopollenin in Vascular Plants, Molecular Plant (2020), https://doi.org/10.1016/j.molp.2020.08.005

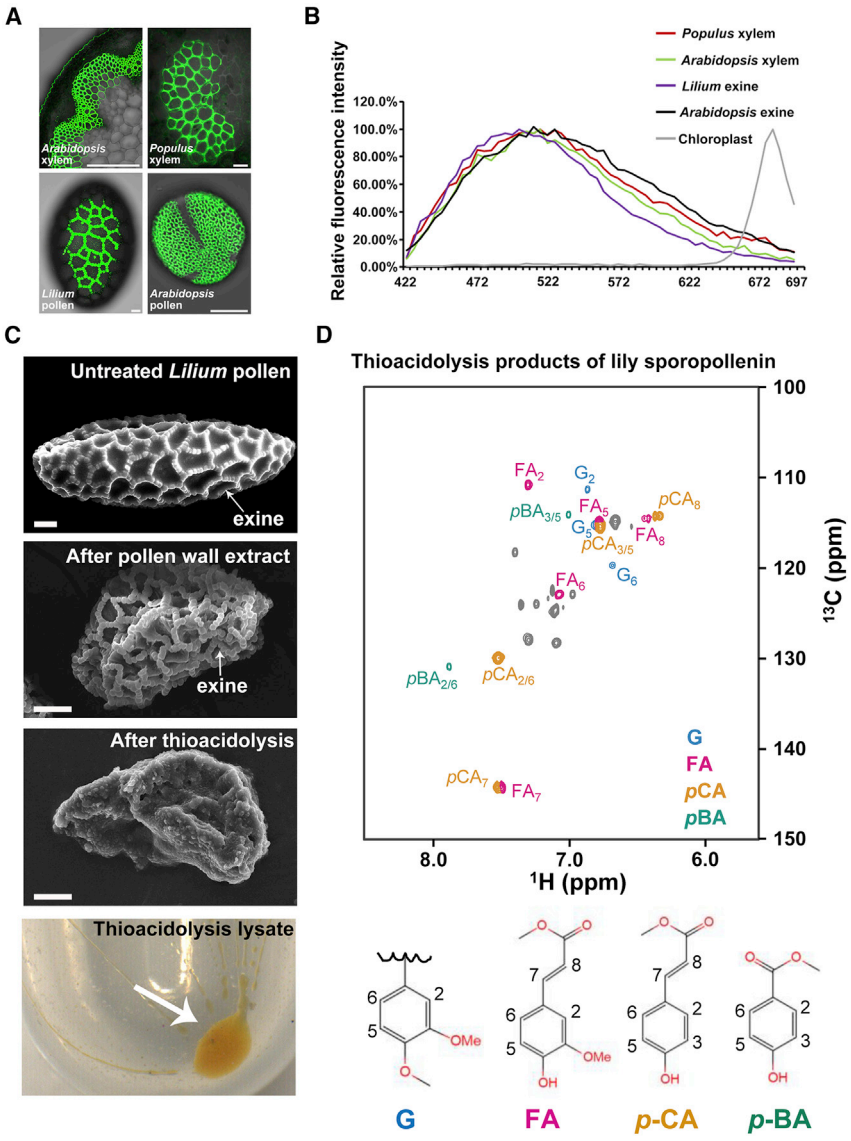

Figure 1. *Lilium* Sporopollenin Contains Derivatives from the Phenylpropanoid Pathway.

(A) Autofluorescence of the xylem cell wall and pollen wall. Left to right: *Arabidopsis* xylem, *Populus* xylem, scale bars correspond to 50 μm. *Lilium* pollen wall, *Arabidopsis* pollen wall, scale bars correspond to 10 μm.

(B) Wavelength scans of pollen exine and xylem cell walls obtained using *laser scanning confocal microscopy*. The maximum emission wavelength was artificially defined as 100%.

(C) Scanning electron micrographs of *Lilium brownii* pollen grains. The untreated (upper), organic solvent-extracted (middle), and thioacidolyzed (bottom) pollen grains were visualized by scanning electron microscopy. Scale bars correspond to 10 μm. The oil-like lysis product of thioacidolysis obtained after blow drying under N_2 is shown in the bottom-most panel. The arrow shows the lysis product.

(D) Partial NMR spectra of the thioacidolysis products of *Lilium* sporopollenin, showing the aromatic signals of phenylpropanoids. A diagram of the detected phenylpropanoids is shown at the bottom.

Figures 2–4); thus, their expression is closely correlated with the stages of exine formation (Blackmore et al., 2007; Wang et al., 2018). However, the expression of *COMT* and *F5H*, which are essential for the synthesis of the S unit of lignin (Chapple et al., 1992; Li et al., 2000; Goujon et al., 2003; Bonawitz and Chapple, 2010), was not detected in the tapetum (Figure 2A). This result is consistent with the fact that the S unit was not detected in the lysate of sporopollenin (Figure 1D). Taken together, these results demonstrate that the phenylpropanoid pathway is expressed in the tapetum, which is consistent with the presence of the G unit, *p*-BA, *p*-CA, and FA in pollen walls.

The Phenylpropanoid Pathway Is Required for Pollen Wall Formation

Phenylpropanoid-deficient mutants, including *pal1 pal2 pal3 pal4* (Huang et al., 2010), *ref3-1* and *ref3-2* (*C4H* gene mutants) (Schilmiller et al., 2009), *4cl1 4cl2 4cl3* (*4cl tm*) (Li et al., 2015), and *ccr1* (Thevenin et al., 2011), show compromised fertility. To examine whether the reduced fertility is related to pollen wall formation, we analyzed the pollen phenotypes of several mutants, including those resulting from two strong alleles, *4cl tm* and *ref3-2*, and two weak alleles, *ref3-1* and *ccr1-4* (point mutations). No viable pollen grains were found in *4cl tm* or *ref3-2* (Figure 2B) (Schilmiller et al., 2009). In *ref3-2*, all the defective pollen grains were stuck together in the anther locules, and a reticulate exine with distinct baculae and tecta was not detected (Supplemental Figure 5). There are four *4CL* genes in *Arabidopsis* (Li et al., 2015). In *4cl tm*, many defective pollen grains were stuck together and the reticulate exine was lost (Figure 2B and Supplemental Figure 6). Together, the phenotypes of *ref3-2* and *4cl tm* are similar to those of plants with strong mutant alleles of enzymes involved in aliphatic modification in the sporopollenin synthesis pathway (de Azevedo Souza et al., 2009; Kim et al., 2010). In plants homozygous for the *ref3-1* and *ccr1-4* weak alleles, approximately 40% of the pollen was defective (Supplemental Figure 7). Both *ref3-1* and *ccr1-4* have disorganized exine missing baculae and tecta in some areas (Figure 2B and Supplemental Figure 6). This phenotype is similar to that of plants with weak mutant alleles of enzymes involved in aliphatic modification (Morant and Bak, 2007; Dobritsa et al., 2009). Furthermore, the autofluorescence intensity of the defective pollen grains of *4cl tm* and the pollen grains of *ref3-1* and *ccr1-4* was lower than that of wild-type (WT) pollen, which was consistent with the exine abnormalities observed in these mutants (Figure 2B). These genetic analyses demonstrate that the phenylpropanoid pathway is essential for exine formation (Figure 2C). Thus, both sporopollenin

Please cite this article in press as: Xue et al., Phenylpropanoid Derivatives Are Essential Components of Sporopollenin in Vascular Plants, Molecular Plant (2020), https://doi.org/10.1016/j.molp.2020.08.005

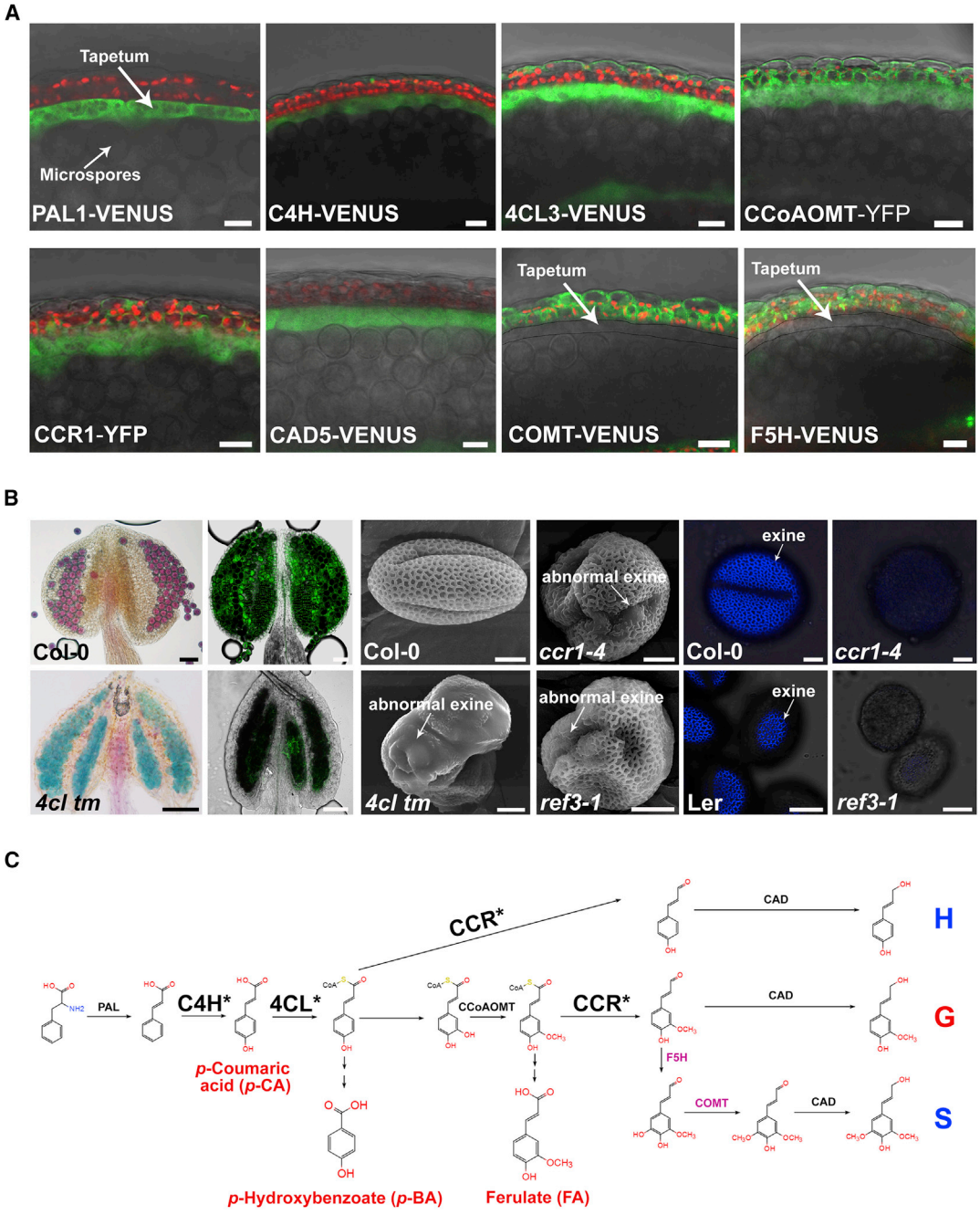

Figure 2. The Phenylpropanoid Pathway Is Required for Sporopollenin Biosynthesis.

(A) Expression of *PAL1*, *C4H*, *4CL3*, *CCoAOMT*, *CCR1*, *CAD5*, *COMT*, and *F5H* in anthers of *Arabidopsis* after anther stage 7. *COMT* and *F5H* were not expressed in the tapetum. The VENUS and YFP signals are colored green, and the chloroplasts are colored red. Scale bars correspond to 10 μm.

(B) The lignin synthesis mutants had defective pollen exine and defective autofluorescence. Results from Alexander's staining of Col-0 and the *4cl* triple mutant are shown in the first column on the left; images of anther lignin autofluorescence of Col-0 and *4cl tm* are shown in the second column. Scale bars correspond to 50 μm. Scanning electron microscopy images of Col-0, *4cl tm*, *ccr1-4*, and *ref3-1* are shown in the third and fourth columns. Scale bars correspond to 10 μm. Images of pollen lignin autofluorescence of Col-0, Landsberg *erecta* (Ler), *ccr1-4*, and *ref3-1* are shown in the fifth and sixth columns. Scale bars correspond to 10 μm. The arrows indicate normal or abnormal exine.

(C) Summary of molecules identified in sporopollenin, phenylpropanoid pathway genes expressed in the tapetum, and mutants with defective sporopollenin. The simplified phenylpropanoid pathway was modified from that of Boerjan et al. (2003) and Soubeyrand et al. (2018).

Red text: molecules identified in sporopollenin. Blue text: molecules not detected in sporopollenin. Black text: enzymes detected in the tapetum. Pink text: enzymes not detected in the tapetum. The asterisks and large text: mutants with defective sporopollenin.

Please cite this article in press as: Xue et al., Phenylpropanoid Derivatives Are Essential Components of Sporopollenin in Vascular Plants, Molecular Plant (2020), https://doi.org/10.1016/j.molp.2020.08.005

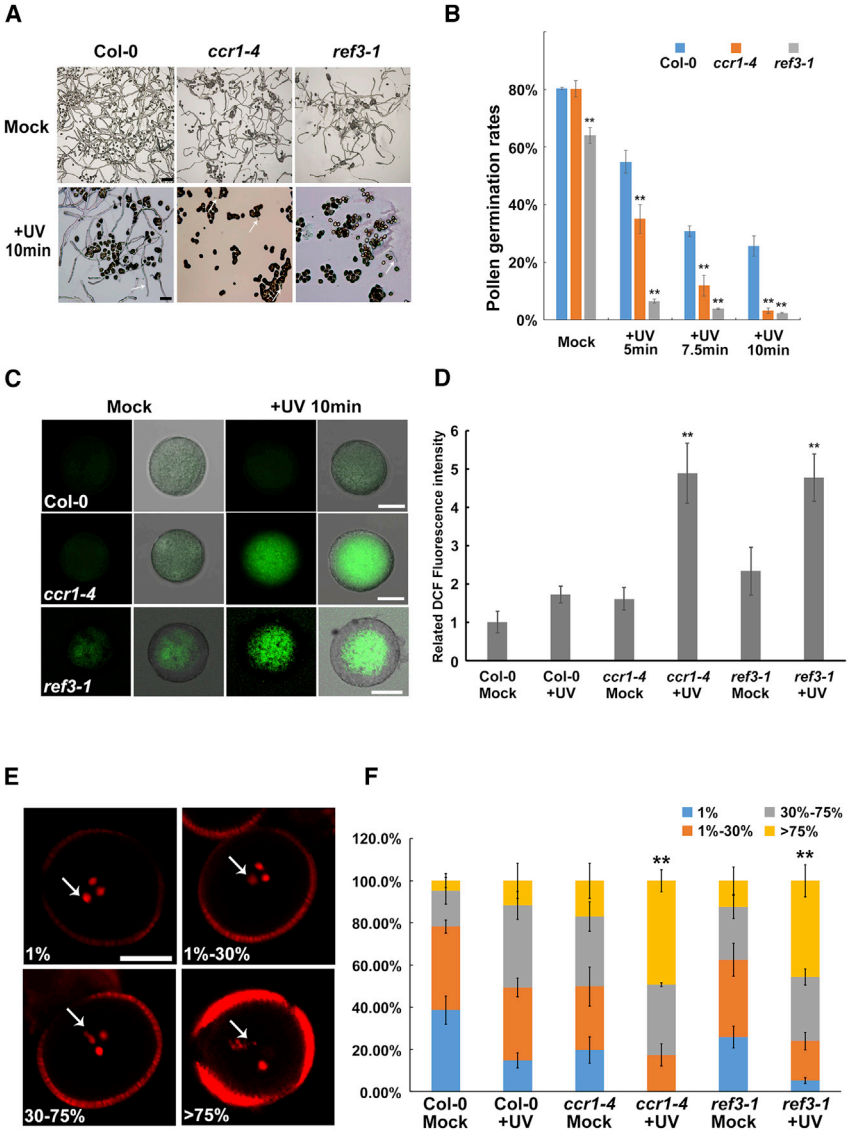

Figure 3. Phenylpropanoid Derivatives in Sporopollenin Protect Pollen from UV Damage.

(A) *ref3-1* and *ccr1-4* were hypersensitive to UV treatment. Pollen treated with 302 nm UV light (Tanon, UV-100) for different durations. Scale bars correspond to 50 μm (for the mock treatment) and 20 μm (for the UV treatment). The arrows indicate the pollen tube.

(B) Statistical analysis of germination rates after UV-B treatment. The data were visualized using Excel (n = 3). Two-way ANOVA showed that the interaction of UV response and *ccr1* and *ref3* mutant was significant ($P < 0.01$), indicating that *ref3-1* and *ccr1* were hypersensitive to the UV treatment. The asterisks indicate statistically significant differences compared with Col-0 ($P < 0.01$) (pairwise t-test, using t-tests with pooled SDs).

(C) Analysis of ROS in the *ccr1* and *ref3-1* pollen after UV treatment. The first column in the mock and UV treatment images shows the ROS signals only. The second column shows the merged images of the image in the first column and the corresponding bright-field image.

(D) Statistical analysis of the ROS content. The data were visualized using Excel (n = 5). Two-way ANOVA showed that the interaction of UV response and the *ccr1* and *ref3-1* mutant was significant ($P < 0.01$). The asterisks indicate statistically significant differences compared with the mock-treated *ccr1* ($P < 0.01$, Tukey's honestly significant difference test).

(E and F) DNA damage greatly increased in the *ccr1* and *ref3-1* mutants after UV treatment. **(E)** Representative images of four arbitrarily determined classes of DNA damage: Nuclei with little or no DNA in the tails were defined as 1%, less than 30% DNA in tails as 1%–30%, 30%–75% DNA in tails as 30%–75%, and almost all the DNA in tails as >75%.

(F) Frequency distribution of the classes of DNA damage in Col-0, *ref3-1*, and *ccr1-4* after UV treatment. The data represent the means ± SDs (n = 3). The type of >75% highly accumulated in UV-treated *ccr1-4* and *ref3-1* pollen. Two-way ANOVA was performed. The interaction of UV response and the *ccr1* and *ref3-1* mutants was significant ($P < 0.01$).

and lignin share the same phenylpropanoid pathway in *Arabidopsis*.

Phenylpropanoid Derivatives Provide UV Protection for Pollen

Phenylpropanoid derivatives are UV-absorbing compounds (Vogt, 2010). Pollen grains have been demonstrated to be resistant to radiation (Brewbaker and Emery, 1961; Fabergé, 1957; Torabinejad et al., 1998). The sporopollenin wall is known to absorb UV and protect pollen protoplasm (Rozema et al., 2001), but the components of sporopollenin responsible for this are not clear (Mikhael et al., 2020; Rozema et al., 2001). We compared pollen germination between WT Col-0, *ref3-1*, and the *ccr1-4* mutant under UV radiation. Under UV-B (302 nm, 6 W) radiation, the germination rates of *ref3-1* and *ccr1-4* were significantly lower compared with those of the WT plants (Figure 3A, 3B and Supplemental Figure 8). UV radiation is known to damage DNA and produce reactive oxygen species (ROS) (Ahmad, 2017). ROS also play regulatory roles during pollination (Zhang et al., 2020). We further analyzed the ROS content in the WT and *ccr1-4* and *ref3-1* mutants under UV light using dichlorofluorescein (DCF) staining. Strong ROS signals were detected in UV-treated *ccr1-4* and *ref3-1* pollen (Figure 3C and 3D). We further used a comet assay to assess DNA damage (Tice et al., 2000). Only weak DNA damage signals were detected in the WT pollen exposed to UV light for 10 min, whereas DNA damage markedly increased in the *ccr1-4* and *ref3-1* pollen under the same conditions (Figure 3E and 3F). Thus, pollen from plants with defective phenylpropanoid pathway function has compromised UV protection. Exposure to UV radiation is a potentially catastrophic event for both pollen and spores of land plants. These results further indicate that

Please cite this article in press as: Xue et al., Phenylpropanoid Derivatives Are Essential Components of Sporopollenin in Vascular Plants, Molecular Plant (2020), https://doi.org/10.1016/j.molp.2020.08.005

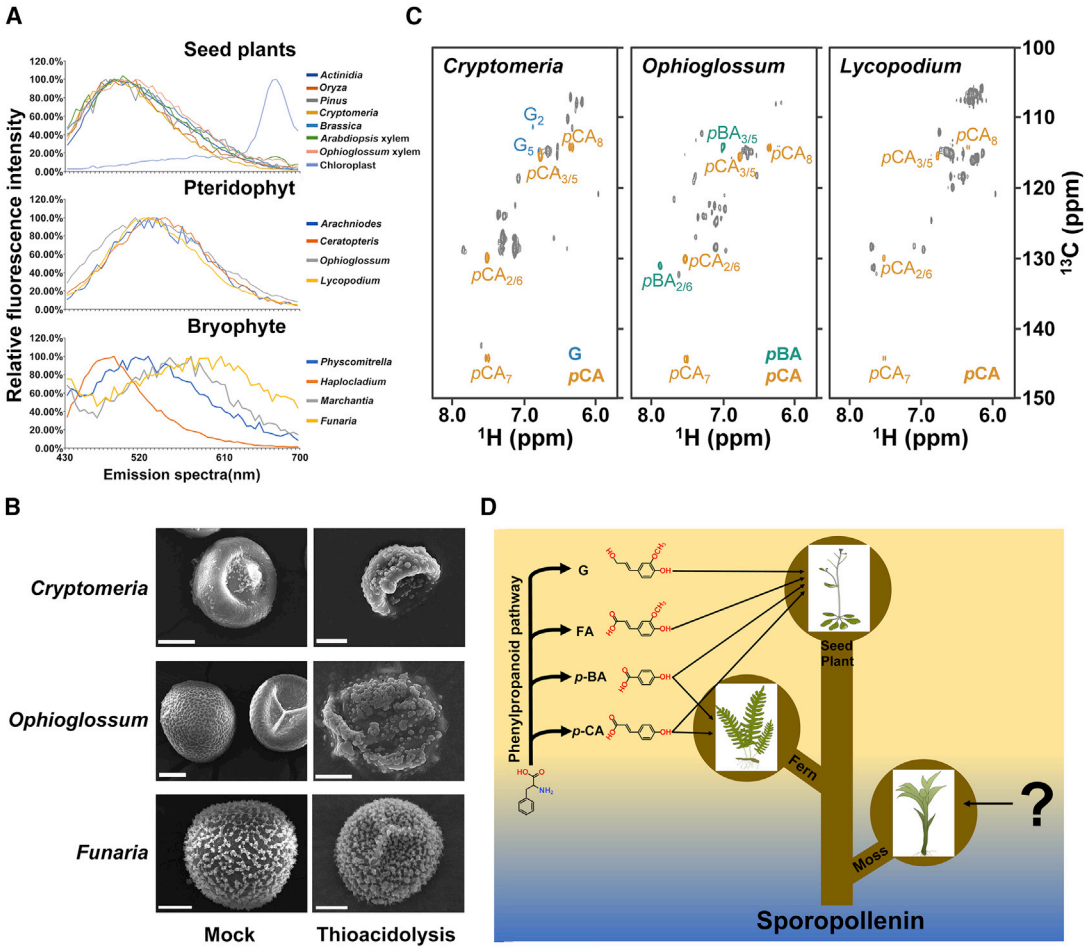

Figure 4. Phenylpropanoid Derivatives Are Present in the Sporopollenin of Vascular Plants.

(A) Results of *laser scanning confocal microscopy* wavelength scans of pollen and spore exine. In seed plants, all the autofluorescence wavelengths were similar. The maximum emission wavelength was 500 nm. In pteridophytes, the wavelengths were also similar, and the maximum emission wavelength was 545 nm.

(B) Thioacidolysis degraded the sporopollenin of both pollen and spores in vascular plants. However, thioacidolysis did not degrade the sporopollenin layer of bryophyte spores. Scale bars correspond to 10 μm.

(C) Partial NMR spectra of the thioacidolysis products of *Cryptomeria*, *Ophioglossum*, and *Lycopodium* sporopollenin, showing the aromatic signals of phenylpropanoids. The detected phenylpropanoids were *p*-CA and G units in *Cryptomeria*, *p*-BA, and *p*-CA in *Ophioglossum*, and *p*-CA in *Lycopodium*.

(D) A proposed model deciphering that the products of the phenylpropanoid pathway are components of sporopollenin in vascular plants.

phenylpropanoid derivatives are crucial for maintenance of the genomic integrity of pollen.

Phenylpropanoid Derivatives Are Present in the Sporopollenin of Vascular Plants

Land plants are divided into seed plants, pteridophytes, and bryophytes. Both seed plants and pteridophytes contain lignin in their vascular tissues and are termed vascular plants. Sporopollenin is considered to be a synapomorphy of land plants (Wellman, 2004; Fraser et al., 2012). We analyzed the sporopollenin composition in a variety of seed plants (*Actinidia*, *Oryza*, *Brassica*, *Pinus*, *Cryptomeria*), pteridophytes (*Ceratopteris*, *Ophioglossum*, *Lycopodium*, *Arachniodes*), and bryophytes (*Physcomitrella*, *Haplocladium*, *Marchantia*, *Funaria*) (Figure 4A). Exine autofluorescence was detected in all of the pollen and spores of these plants (Supplemental Figure 9). Furthermore, wavelength scans showed that the autofluorescence spectra of all the seed plants (five angiosperms and two gymnosperms) are similar, with a maximum emission of approximately 500 nm (Figure 4A). Although the autofluorescence spectra of sporopollenin were similar among all the pteridophyte species, the maximum emission wavelength of these species was approximately 540 nm, which was different from that of the seed plants (Figure 4A). In bryophytes, the sporopollenin autofluorescence spectra differed among *Physcomitrella*, *Haplocladium*, *Funaria*, and *Marchantia* (Figure 4A). These findings suggest that, in bryophytes, different molecules may be involved in sporopollenin formation.

We performed thioacidolysis to analyze the sporopollenin composition of the pollen of *Actinidia* (a dicotyledon), *Oryza* and *Zea mays* (monocotyledons), *Cryptomeria* (a gymnosperm), and of the spores of *Ophioglossum* and *Lycopodium* (pteridophytes). All the sporopollenin of these pollen and spores was degraded

Please cite this article in press as: Xue et al., Phenylpropanoid Derivatives Are Essential Components of Sporopollenin in Vascular Plants, Molecular Plant (2020), https://doi.org/10.1016/j.molp.2020.08.005

after thioacidolysis (Figure 4B and Supplemental Figure 10). However, in the bryophytes *Haplocladium* and *Funaria*, the exine layer was not dissolved by thioacidolysis (Figure 4B and Supplemental Figure 10). HSQC NMR analysis showed that the G unit and *p*-CA were present in *Cryptomeria* (Figure 4C), and these compounds were also identified in *Lilium* sporopollenin (Figure 1). The similarity of emission spectra of exine autofluorescence (Figure 4A) suggests that seed plant sporopollenin contains both the G unit and hydroxycinnamates of the phenylpropanoid pathway. In the sporopollenin of *Ophioglossum* and *Lycopodium* (pteridophytes), *p*-BA and *p*-CA but not the lignin G unit were detected (Figure 4C). This shows that the sporopollenin composition of pteridophytes is different from that of seed plants. However, vascular plants, including both seed plants and pteridophytes, contain phenylpropanoid derivatives in their sporopollenin. Taken together, these results indicate that the composition of sporopollenin varies among land plants.

The sporopollenin wall enclosing pollen and spores is considered to be an essential protective structure of plants for dispersal in subaerial conditions (Wellman, 2004). Its composition has intrigued scientists for decades (Holt and Bennett, 2014). Genetic and biochemical analyses indicate that aliphatic units are components of sporopollenin in seed plants (Ariizumi and Toriyama, 2010; Quilichini et al., 2015). However, whether phenolic compounds are present in sporopollenin remains under debate (Li et al., 2019; Mikhael et al., 2020). In this work, we demonstrated through biochemical, cytological, and genetic analyses that phenylpropanoid derivatives, including lignin G units, *p*-CA, *p*-BA, and FA, are essential components of sporopollenin (Figures 1 and 2). Exposure to UV radiation is potentially catastrophic for the pollen of land plants. Sporopollenin absorbs UV and protects pollen (Rozema et al., 2001). Our results showed that a defective phenylpropanoid pathway weakens the UV resistance of pollen, indicating its function in UV protection and maintenance of pollen genomic integrity (Figure 3).

Both sporopollenin and lignin contain derivatives of the phenylpropanoid pathway. Pteridophyte lignin is mainly composed of G units (Weng and Chapple, 2010). However, only *p*-CA and *p*-BA are integrated in the sporopollenin (Figure 4). Early seed plants (gymnosperms) emerged approximately 330 million years ago (Magallon et al., 2013). Gymnosperm lignin is also typically composed of G units (Ros et al., 2007), and gymnosperm sporopollenin contains G units and hydroxycinnamates (Figure 4). Angiosperms became established approximately 190 million years ago (Magallon et al., 2013). Both G and S units are abundant in angiosperm lignin (Ros et al., 2007), but only G units are present in the sporopollenin (Figure 1). The rise of vascular plants, which have developed the ability to deposit lignin in the cell wall, significantly affected terrestrial ecosystems (Weng and Chapple, 2010). We show that the synthesis of both sporopollenin and lignin occurs via the phenylpropanoid pathway in vascular plants (Figures 1 and 4). Future investigations of the role of the phenylpropanoid pathway in the synthesis of sporopollenin and lignin may provide an improved understanding of plant evolution in terrestrial environments.

METHODS

Plant Materials and Growth Conditions

The *ccr1-4* (Xue et al., 2015), *4cl tm* (Li et al., 2015), *ref3-2*, and *ref3-1* (Schilmiller et al., 2009) mutants have been described previously. The plants were grown under long-day conditions (16 h light/8 h darkness) in an ~22°C growth chamber. *Lilium brownii* flowers were obtained from the Shanghai Qingqing (China) flower company. Pollen of *Actinidia sinensis* was ordered from the Anhui Nongliteng (China) seed company. Pollen of *Zea mays* was provided by Yongrui Wu (Chinese Academic of Science). Pollen of *Oryza sativa*, *Brassica juncea*, *Pinus kwangtungensis*, and *Cryptomeria fortune*, and spores of *Ophioglossum vulgatum*, *Arachniodes exilis*, *Ceratopteris thalictroides*, *Physcomitrella patens*, *Haplocladium microphyllum*, and *Funaria hygrometrica* were collected from Shanghai Normal University. *Lycopodium clavatum* spores were obtained from Sigma (19108-100G-F). Spores of *Marchantia polymorpha* were provided by Yue Sun (East China Normal University). A UV light (UV-100) was obtained from Tanon Science & Technology, China.

Histology and Microscopy

Alexander's solution was prepared as described previously (Alexander, 1969). Anthers were dissected and immersed in Alexander's solution for 1 h, and images were obtained under a microscope with an Olympus BX51 digital camera (Olympus, Japan).

Scanning Electron Microscopy

Individual pollen grains were collected from freshly dehisced anthers. Pollen grains were mounted on scanning electron microscopy stubs, and the mounted samples were then coated with palladium-gold in a sputter coater (pattern) and examined by scanning electron microscopy (JSM-840; JEOL, http://www.jeol.com) with an acceleration voltage of 15 kV. For transmission electron microscopy observation, *Arabidopsis* buds from inflorescences were fixed in 0.1 M phosphate buffer (pH 7.2) consisting of 2.5% glutaraldehyde (v/v), and then washed several times before being dehydrated through a series of acetone/water mixtures. Finally, the flower buds were embedded into fresh mixed resin and polymerized into molds. Ultrathin sections (70–100 nm thick) were observed using transmission electron microscopy (JEOL, Japan).

Confocal Microscopy

Images were obtained with an Olympus FV3000 laser scanning microscope. For wavelength scans, we used 405 nm for excitation, and emission spectra were recorded in the range of 420–700 nm. The bandwidth was set to 10 nm. Spectra of chloroplasts, xylem, and exine were recorded under these conditions. For lignin autofluorescence, we used 405 nm for excitation, and emission spectra were recorded in the range of 450–550 nm. Water was used as mounting media. z stack scanning was performed to generate 3D images of the pollen grains. Orthogonal views of the 3D confocal microscopy images were obtained. To monitor YFP/VENUS fluorescence using confocal microscopy, a 514-nm laser line was used for excitation, and a 525- to 570-nm bandpass filter was used for detection. Three independent transgenic lines of each construct were analyzed and showed the same expression pattern. For chloroplast fluorescence, a 514-nm laser was used for excitation, and a 650- to 750-nm bandpass filter was used for detection.

UV Treatment, ROS Staining, and Comet Assays

In brief, pollen grains of *Arabidopsis* were collected, spread onto glass slides or dishes, and then treated with UV for 5–10 min. The UV lamp (6 W) was placed 5 mm above the slides or dishes. For the pollen germination assays, more than 30 pollen grains were counted each time, and three biological repeats were included. The DCF staining method was applied as described previously (Xue et al., 2015). Pollen grains after the treatment were washed and then stained with DCF solution for 10 min. The fluorescence was analyzed using an FV3000 laser scanning microscope. We used 488 nm for excitation, and the emission spectra

Please cite this article in press as: Xue et al., Phenylpropanoid Derivatives Are Essential Components of Sporopollenin in Vascular Plants, Molecular Plant (2020), https://doi.org/10.1016/j.molp.2020.08.005

were recorded in the range of 498–532 nm. Comet assays were applied as described previously (Luo et al., 2012). In brief, pollen grains of *Arabidopsis* were collected and spread onto glass slides and treated with UV. Then, pollen grains were washed and resuspended in low-melting point agarose, which was then spread onto glass slides. After the agarose solidified, the glass slides were immersed in lysis buffer and alkaline buffer to remove the cell membranes and proteins. Finally, the glass slides were electrophoresed for 10 min, and the DNA fragments moved faster than the intact chromosomes did. The DNA was subsequently stained by propidium iodide and analyzed using an FV3000 laser scanning microscope.

Pollen Wall Collection and Thioacidolysis

In brief, pollen grains were isolated and treated with 70% ethanol for 1 h. The insoluble residue was collected, washed with 1.5 ml of chloroform:methanol (1:1), and then centrifuged at 10 000 rpm. The chloroform:methanol (1:1) wash step was repeated three times. Insoluble residue from the chloroform:methanol (1:1) step was then washed three times with 1 ml of acetone, and the solvent was evaporated at 35°C until it was dry. One-gram dry pellets was resuspended in 15 ml of 0.1 M sodium acetate buffer (pH 5.0) and heated at 80°C for 20 min, after which the resuspended pellet was treated with 350 μl of sodium azide (0.01%), 350 μl of amylase (Sigma) (50 μg/ml), and 170 μl of pullulanase (Sigma) (17.8 units) and then incubated overnight at 37°C in a shaker. The reactions were terminated by heating the suspension at 100°C for 10 min, after which the mixture was centrifuged to collect the insoluble residue, which comprised pollen walls. The remaining pellet was washed three times with 1.5 ml of water and an additional three times with 200 μl of acetone and air dried to produce the final cell wall material. For thioacidolysis, the prepared 0.5-g cell wall material was derivatized as described previously (Foster et al., 2010).

NMR Analysis

NMR spectroscopy analyses were performed using an Agilent DD2 600-MHz NMR spectrometer. The proton and 2D NMR spectra were acquired at 298 K with a gradient 5-mm $^{1}H/^{13}C/^{15}N$ triple-resonance cold probe as described previously (Zhang et al., 2017). For HSQC analysis, the thioacidolysis product from approximately 50 mg of pollen grains was dissolved in 0.6 ml of deuterated DMSO-*d6* (99.9%, Sigma). The standard pulse sequence gHSQCAD was used to determine the one-bond ^{1}H-^{13}C correlation in samples. The ^{1}H-^{13}C HSQC spectra were collected using a spectrum width of 10 ppm in the F2 (^{1}H) dimension and 200 ppm in the F1 (^{13}C) dimension. The 1024 × 256 (F2 × F1) complex data points were collected with the receiver gain set to 30. For the total correlation spectroscopy analysis, the experiments were conducted using the standard pulse sequence total correlation spectroscopy method. These spectra were calibrated using the DMSO solvent peak (dC 39.5 ppm and dH 2.49 ppm). All spectrum processing was performed using Mest ReNova 10.0.2 software.

The assignment of signals in the aromatic regions of HSQC spectra of thioacidolysis lysates was performed according to a previous report, where the NMR spectra of cell wall lignins were characterized (Karlen et al., 2018). Based on the characteristic signals of the phenylpropanoid derivatives, we identified the chemical shifts of the G lignin unit: C2H (111.16 ppm, 6.87 ppm), C5H (115.14 ppm, 6.82 ppm), C6H (119.60 ppm, 6.68 ppm); *p*-CA: C2H (110.59 ppm, 7.31 ppm), C5H (114.49 ppm, 6.78 ppm), C6H (122.72 ppm, 7.08 ppm), C7H (144.27 ppm, 7.49 ppm), C8H (114.27 ppm, 6.42 ppm); FA: C2/6H (129.83 ppm, 7.52 ppm), C3/5H (115.24 ppm, 6.78 ppm), C7H (144.26 ppm, 7.53 ppm), C8H (114.11 ppm, 6.34 ppm); and *p*-BA: C2/6H (130.85 ppm, 7.88 ppm), C3/5H (113.97 ppm, 7.01 ppm). These chemical signals are labeled in the corresponding Figures and Figure legends.

Plasmid Construction and Plant Transformation

To generate *ProCCR1::CCR1-YFP* constructs, we replaced the GUS DNA sequence of *ProCCR1::CCR1-GUS* with the gene encoding YFP (Xue et al., 2015). The resulting construct was named *ProCCR1::CCR1-YFP*. To generate the *ProPAL1::PAL1*-VENUS, *ProC4H*::*C4H*-VENUS, *Pro4CL3*::*4CL3*-VENUS, *ProCAD4*::*CAD4*-VENUS, *ProCAD5*::*CAD5*-VENUS, *ProCCoAOMT*::*CCoAOMT*-VENUS, *ProCOMT*::*COMT*-VENUS, and *ProF5H*::*F5H*-VENUS constructs, the genomic DNA sequences of *PAL1*, *C4H*, *4CL3*, *CCoAOMT*, *COMT*, *F5H*, *CAD4*, and *CAD5* were ligated into the P1300-VENUS plasmid using the pEASY-Uni Seamless Cloning and Assembly Kit (Yao et al., 2018). For plant transformation, the plasmid was introduced into *Agrobacterium* strain GV3101 and transformed into plants using the floral dip method (Clough and Bent, 2010).

Pollen Germination Assays

The pollen germination assay was performed as described previously (Hai et al., 1999). In brief, pollen grains of *Arabidopsis* were collected and spread on germination media and treated with UV exposure or a mock treatment. The pollen was germinated at 24°C for 16 h and then examined under a light microscope with an Olympus BX51 digital camera.

ACCESSION NUMBERS

The accession numbers for the studied genes are as follows: PAL1 (AT2G37040), C4H (AT2G30490), 4CL1 (AT1G51680), 4CL2 (AT3G21420), 4CL3 (AT1G65060), *CCR1* (AT1G15950), CAD4 (AT3G19540), CAD5 (AT4G34230), CCoAOMT (AT4G34050), COMT (AT5G54160), and F5H (AT4G36220).

SUPPLEMENTAL INFORMATION

Supplemental Information is available at *Molecular Plant Online*.

FUNDING

This work was supported by grants from the National Key Research and Development Program of China (2016YFD0100902), the National Natural Science Foundation of China (31900165, 31870296, 31700277), the Strategic Priority Research Program of the Chinese Academy of Sciences (XDB27020104), the Program from Shanghai Municipal Education Commission [2019-01-07-00-02-E00006], the China Postdoctoral Science Foundation (2017M61159), and Jiangsu Collaborative Innovation Center for Modern Crop Production (to H.D.Z.).

AUTHOR CONTRIBUTIONS

The experiments were conceived and designed by Z.-N.Y., J.-S.X., and H.D.Z. The experiments were performed by J.-S.X., B.Z., Y.-L.L., X.-L.J., H.D.Z., T.H.W., Y.-X.L., W.-J.H., and N.-Y.Y. The data were analyzed by J.-S.X., B.Z., H.D.Z., J.-S.G., L.L., J.-F.H., and Z.-N.Y. The paper was written by J.-S.X., Z.-N.Y., P.X., L.L., Y.Z., Z.-B.Z., and J.C. All the authors have read the manuscript and approved it for submission.

ACKNOWLEDGMENTS

We thank Clint Chapple and Peng Wang for providing seeds of *4cl tm*, Xiaoshu Gao for confocal microscopy analysis, and Shuming Cao for providing *Populus* samples. We also thank Gregory P. Copenhaver (UNC Chapel Hill), Lu Bao-Rong (Fudan University), Jeremy Murray (Institute of Plant Physiology & Ecology, Chinese Academy of Sciences), and Huang Hai for assistance in editing the manuscript before submission. All authors have no conflict of interest.

Received: January 15, 2020
Revised: June 3, 2020
Accepted: August 13, 2020
Published: August 15, 2020

REFERENCES

Aarts, M.G., Hodge, R., Kalantidis, K., Florack, D., Wilson, Z.A., Mulligan, B.J., Stiekema, W.J., Scott, R., and Pereira, A. (1997). The *Arabidopsis* MALE STERILITY 2 protein shares similarity with

reductases in elongation/condensation complexes. Plant J. **12**:615–623.

S.I. Ahmad, ed. (2017). Ultraviolet Light in Human Health, Diseases and Environment. Advances in Experimental Medicine and Biology, 996 (Cham: Springer).

Alexander, M.P. (1969). Differential staining of aborted and nonaborted pollen. Stain Technol. **44**:117–122.

Ariizumi, T., and Toriyama, K. (2010). Genetic regulation of sporopollenin synthesis and pollen exine development. Annu. Rev. Plant Biol. **62**:437–460.

Blackmore, S., Wortley, A.H., Skvarla, J.J., and Rowley, J.R. (2007). Pollen wall development in flowering plants. New Phytol. **174**:483–498.

Boerjan, W., Ralph, J., and Baucher, M. (2003). Lignin biosynthesis. Annu. Rev. Plant Biol. **54**:514–594.

Bonawitz, N.D., and Chapple, C. (2010). The genetics of lignin biosynthesis: connecting genotype to phenotype. Annu. Rev. Genet. **44**:337–363.

Brewbaker, J.L., and Emery, G.C. (1961). Pollen radiobotany. Radiat. Bot. **1**:101–154.

Brooks, J., and Shaw, G. (1968). Chemical structure of the exine of pollen walls and a new function for carotenoids in nature. Nature **219**:532–533.

Brooks, J., and Shaw, G. (1978). Sporopollenin: a review of its chemistry, palaeochemistry and geochemistry. Grana **17**:91–97.

Bubert, H., Lambert, J., Steuernagel, S., Ahlers, F., and Wiermann, R. (2002). Continuous decomposition of sporopollenin from pollen of *Typha angustifolia* L. by acidic methanolysis. Z. Naturforsch. C **57**:1035–1041.

Chang, F., Wang, Y., Wang, S., and Ma, H. (2011). Molecular control of microsporogenesis in *Arabidopsis*. Curr. Opin. Plant Biol. **14**:66–73.

Chapple, C.C., Vogt, T., Ellis, B.E., and Somerville, C.R. (1992). An *Arabidopsis* mutant defective in the general phenylpropanoid pathway. Plant Cell **4**:1413–1424.

Clough, S.J., and Bent, A.F. (2010). Floral dip: a simplified method for *Agrobacterium*-mediated transformation of *Arabidopsis thaliana*. Plant J. **16**:735–743.

Crang, R.E., and May, G. (1974). Evidence for silicon as a prevalent elemental component in pollen wall structure. Can. J. Bot. **52**:2171–2174.

de Azevedo Souza, C., Kim, S.S., Koch, S., Kienow, L., Schneider, K., McKim, S.M., Haughn, G.W., Kombrink, E., and Douglas, C.J. (2009). A novel fatty Acyl-CoA Synthetase is required for pollen development and sporopollenin biosynthesis in *Arabidopsis*. Plant Cell **21**:507–525.

Derikvand, M., Sierra, J., Ruel, K., Pollet, B., Do, C., Thévenin, J., Buffard, D., Jouanin, L., and Lapierre, C. (2008). Redirection of the phenylpropanoid pathway to feruloyl malate in *Arabidopsis* mutants deficient for cinnamoyl-CoA reductase 1. Planta **227**:943–956.

Dobritsa, A.A., Shrestha, J., Morant, M., Pinot, F., Matsuno, M., Swanson, R., Moller, B.L., and Preuss, D. (2009). CYP704B1 is a long-chain fatty acid ω-hydroxylase essential for sporopollenin synthesis in pollen of *Arabidopsis*. Plant Physiol. **151**:574–589.

Dobritsa, A.A., Lei, Z., Nishikawa, S., Urbanczyk-Wochniak, E., Huhman, D.V., Preuss, D., and Sumner, L.W. (2010). LAP5 and LAP6 encode anther-specific proteins with similarity to chalcone synthase essential for pollen exine development in *Arabidopsis*. Plant Physiol. **153**:937–955.

Dobritsa, A.A., Geanconteri, A., Shrestha, J., Carlson, A., Kooyers, N., Coerper, D., Urbanczyk-Wochniak, E., Bench, B.J., Sumner, L.W., Swanson, R., et al. (2011). A large-scale genetic screen in *Arabidopsis* to identify genes involved in pollen exine production. Plant Physiol. **157**:947–970.

Domínguez, E., Mercado, J.A., Quesada, M.A., and Heredia, A. (1999). Pollen sporopollenin: degradation and structural elucidation. Sex. Plant Reprod. **12**:171–178.

Fabergé, A.C. (1957). A method for treating wheat pollen with ultraviolet radiation for genetic experiments. Genetics **42**:618–622.

Foster, C.E., Martin, T.M., and Pauly, M. (2010). Comprehensive compositional analysis of plant cell walls (lignocellulosic biomass) part I: lignin. J. Vis. Exp. **37**:1745.

Fraser, W.T., Scott, A.C., Forbes, A.E., Glasspool, I.J., Plotnick, R.E., Kenig, F., and Lomax, B.H. (2012). Evolutionary stasis of sporopollenin biochemistry revealed by unaltered Pennsylvanian spores. New Phytol. **196**:397–401.

Goujon, T., Sibout, R., Pollet, B., Maba, B., Nussaume, L., Bechtold, N., Lu, F., Ralph, J., Mila, I., Barriere, Y., et al. (2003). A new *Arabidopsis thaliana* mutant deficient in the expression of *O*-methyltransferase impacts lignins and sinapoyl esters. Plant Mol. Biol. **51**:973–989.

Grienenberger, E., Kim, S.S., Lallemand, B., Geoffroy, P., Heintz, D., Souza Cde, A., Heitz, T., Douglas, C.J., and Legrand, M. (2010). Analysis of TETRAKETIDE α-PYRONE REDUCTASE function in *Arabidopsis thaliana* reveals a previously unknown, but conserved, biochemical pathway in sporopollenin monomer biosynthesis. Plant Cell **22**:4067–4083.

Guilford, W.J., Schneider, D.M., Labovitz, J., and Opella, S.J. (1988). High resolution solid state ^{13}C NMR spectroscopy of sporopollenins from different plant taxa. Plant Physiol. **86**:134–136.

Hai, L., Lin, Y.K., Heath, R.M., Zhu, M.X., and Yang, Z.B. (1999). Control of pollen tube tip growth by a rop GTPase-dependent pathway that leads to tip-localized calcium influx. Plant Cell **11**:1731–1742.

Hatfield, R.D., Rancour, D.M., and Marita, J.M. (2016). Grass cell walls: a story of cross-linking. Front. Plant Sci. **7**:2056.

Heslop-Harrison, J. (1962). Origin of exine. Nature **195**:1069–1071.

Holt, K.A., and Bennett, K.D. (2014). Principles and methods for automated palynology. New Phytol. **203**:735–742.

Huang, J., Gu, M., Lai, Z., Fan, B., Shi, K., Zhou, Y.H., Yu, J.Q., and Chen, Z. (2010). Functional analysis of the *Arabidopsis* PAL gene family in plant growth, development, and response to environmental stress. Plant Physiol. **153**:1526–1538.

Karlen, S.D., Free, H.C.A., Padmakshan, D., Smith, B.G., and Harris, P.J. (2018). Commelinid monocotyledon lignins are acylated by p-coumarate. Plant Physiol **177**:513–521.

Kawase, M., and Takahashi, M. (1995). Chemical composition of sporopollenin in *Magnolia grandiflora* (Magnoliaceae) and *Hibiscus syriacus* (Malvaceae). Grana **34**:242–245.

Kim, S.S., Grienenberger, E., Lallemand, B., Colpitts, C.C., Kim, S.Y., Souza Cde, A., Geoffroy, P., Heintz, D., Krahn, D., Kaiser, M., et al. (2010). LAP6/POLYKETIDE SYNTHASE A and LAP5/POLYKETIDE SYNTHASE B encode hydroxyalkyl alpha-pyrone synthases required for pollen development and sporopollenin biosynthesis in *Arabidopsis* thaliana. Plant Cell **22**:4045–4066.

Li, L., Popko, J.L., Umezawa, T., and Chiang, V.L. (2000). 5-Hydroxyconiferyl aldehyde modulates enzymatic methylation for syringyl monolignol formation, a new view of monolignol biosynthesis in angiosperms. J. Biol. Chem. **275**:6537–6545.

Li, H., Pinot, F., Sauveplane, V., Werck-Reichhart, D., and Zhang, D. (2010). Cytochrome P450 family member CYP704B2 catalyzes the ω-hydroxylation of fatty acids and is required for anther cutin biosynthesis and pollen exine formation in rice. Plant Cell **22**:173–190.

Li, Y., Kim, J.I., Pysh, L., and Chapple, C. (2015). Four isoforms of *Arabidopsis* thaliana 4-coumarate: CoA ligase (4CL) have overlapping yet distinct roles in phenylpropanoid metabolism. Plant Physiol. **169**:2409–2421.

Li, F.S., Phyo, P., Jacobowitz, J., Hong, M., and Weng, J.K. (2019). The molecular structure of plant sporopollenin. Nat. Plants **5**:41–46.

Lin, S.Y., and Dence, C.W. (1992). Methods in Lignin Chemistry (Berlin; New York: Springer-Verlag).

Luo, D., Bernard, D.G., Balk, J., Hai, H., and Cui, X. (2012). The *DUF59* family gene *AE7* acts in the cytosolic iron-sulfur cluster assembly pathway to maintain nuclear genome integrity in *Arabidopsis*. Plant Cell **24**:4135–4148.

Magallon, S., Hilu, K.W., and Quandt, D. (2013). Land plant evolutionary timeline: gene effects are secondary to fossil constraints in relaxed clock estimation of age and substitution rates. Am. J. Bot. **100**:556–573.

Mikhael, A., Jurcic, K., Schneider, C., Karr, D., Fisher, G.L., Fridgen, T.D., Diego-Taboada, A., Georghiou, P.E., Mackenzie, G., and Banoub, J. (2020). Demystifying and unravelling the molecular structure of the biopolymer sporopollenin. Rapid Commun. Mass Spectrom. **34**:e8740.

Mitsumoto, K., Yabusaki, K., and Aoyagi, H. (2009). Classification of pollen species using autofluorescence image analysis. J. Biosci. Bioeng. **107**:90–94.

Morant, M., and Bak, S. (2007). CYP703 is an ancient cytochrome P450 in land plants catalyzing in-chain hydroxylation of lauric acid to provide building blocks for sporopollenin synthesis in pollen. Plant Cell **19**:1473–1487.

Osthoff, K.S., and Wiermann, R. (1987). Phenols as integrated compounds of sporopollenin from *Pinus* pollen. J. Plant Physiol. **131**:5–15.

O'Connor, D.J., Iacopino, D., Healy, D.A., O'Sullivan, D., and Sodeau, J.R. (2011). The intrinsic fluorescence spectra of selected pollen and fungal spores. Atmos. Environ. **45**:6451–6458.

Piffanelli, P., Ross, J.H.E., and Murphy, D.J. (1998). Biogenesis and function of the lipidic structures of pollen grains. Plant Reprod. **11**:65–80.

Prahl, A.K., Rittscher, M., and Wiermann, R. (1986). New aspects of sporopollenin biosynthesis. In Biotechnology and Ecology of Pollen, D.L. Mulcahy, G.B. Mulcahy, and E. Ottaviano, eds. (New York: Springer).

Quilichini, T.D., Grienenberger, E., and Douglas, C.J. (2015). The biosynthesis, composition and assembly of the outer pollen wall: a tough case to crack. Phytochemistry **113**:170–182.

Ros, L.V.G., Gabaldón, C., Pomar, F., Merino, F., Pedreño, M.A., and Barceló, A.R. (2007). Structural motifs of syringyl peroxidases predate not only the gymnosperm–angiosperm divergence but also the radiation of tracheophytes. New Phytol. **173**:63–78.

Rozema, J., Broekman, R.A., Blokker, P., Meijkamp, B.B., de Bakker, N., van de Staaij, J., van Beem, A., Ariese, F., and Kars, S.M. (2001). UV-B absorbance and UV-B absorbing compounds (para-coumaric acid) in pollen and sporopollenin: the perspective to track historic UV-B levels. J. Photochem. Photobiol. B **62**:108–117.

Sanders, P.M., Bui, A.Q., Weterings, K., Mcintire, K.N., Hsu, Y.C., Pei, Y.L., Mai, T.T., Beals, T.P., and Goldberg, R.B. (1999). Anther developmental defects in *Arabidopsis thaliana* male-sterile mutants. Sex. Plant Reprod. **11**:297–322.

Schilmiller, A.L., Stout, J., Weng, J.K., Humphreys, J., Ruegger, M.O., and Chapple, C. (2009). Mutations in the *cinnamate 4-hydroxylase* gene impact metabolism, growth and development in *Arabidopsis*. Plant J. **60**:771–782.

Shi, J., Tan, H., Yu, X.-H., Liu, Y., Liang, W., Ranathunge, K., Franke, R.B., Schreiber, L., Wang, Y., and Kai, G. (2011). Defective pollen wall is required for anther and microspore development in rice and encodes a fatty acyl carrier protein reductase. Plant Cell **23**:2225–2246.

Sibout, R., Eudes, A., Mouille, G., Pollet, B., Lapierre, C., Jouanin, L., and Seguin, A. (2005). *CINNAMYL ALCOHOL DEHYDROGENASE-C* and *-D* are the primary genes involved in lignin biosynthesis in the floral stem of *Arabidopsis*. Plant Cell **17**:2059–2076.

Soubeyrand, E., Johnson, T.S., Latimer, S., Block, A., Kim, J., Colquhoun, T.A., Butelli, E., Martin, C., Wilson, M.A., and Basset, G.J. (2018). The peroxidative cleavage of kaempferol contributes to the biosynthesis of the benzenoid moiety of ubiquinone in plants. Plant Cell **30**:2910–2921.

Thevenin, J., Pollet, B., Letarnec, B., Saulnier, L., Gissot, L., Maia-Grondard, A., Lapierre, C., and Jouanin, L. (2011). The simultaneous repression of *CCR* and *CAD*, two enzymes of the lignin biosynthetic pathway, results in sterility and dwarfism in *Arabidopsis thaliana*. Mol. Plant **4**:70–82.

Tice, R.R., Agurell, E., Anderson, D., Burlinson, B., Hartmann, A., Kobayashi, H., Miyamae, Y., Rojas, E., Ryu, J.C., and Sasaki, Y.F. (2000). Single cell gel/comet assay: guidelines for in vitro and in vivo genetic toxicology testing. Environ. Mol. Mutagen. **35**:206–221.

Torabinejad, J., Caldwell, M., Flint, S., and Durham, S. (1998). Susceptibility of pollen to UV-B radiation: an assay of 34 taxa. Am. J. Bot. **85**:360.

Vogt, T. (2010). Phenylpropanoid biosynthesis. Mol. Plant **3**:2–20.

Wang, K., Guo, Z.L., Zhou, W.T., Zhang, C., Zhang, Z.Y., Lou, Y., Xiong, S.X., Yao, X.Z., Fan, J.J., Zhu, J., et al. (2018). The regulation of sporopollenin biosynthesis genes for rapid pollen wall formation. Plant Physiol. **178**:283–294.

Wellman, C.H. (2004). Origin, Function and Development of the Spore Wall in Early Land Plants (London, UK: Royal Botanic Gardens).

Weng, J.K., and Chapple, C. (2010). The origin and evolution of lignin biosynthesis. New Phytol. **187**:273–285.

Willemse, M.T.M. (1972). Changes in the autofluorescence of the pollen wall during microsporogenesis and chemical treatments. Acta Botanica Neerlandica **21**:1–16.

Xu, Z., Zhang, D., Hu, J., Zhou, X., Ye, X., Reichel, K.L., Stewart, N.R., Syrenne, R.D., Yang, X., Gao, P., et al. (2009). Comparative genome analysis of lignin biosynthesis gene families across the plant kingdom. BMC Bioinformatics **10** (*Suppl 11*):S3.

Xue, J., Luo, D., Xu, D., Zeng, M., Cui, X., Li, L., and Huang, H. (2015). *CCR1*, an enzyme required for lignin biosynthesis in *Arabidopsis*, mediates cell proliferation exit for leaf development. Plant J. **83**:375–387.

Yao, X., Yang, H., Zhu, Y., Xue, J., Wang, T., Song, T., Yang, Z., and Wang, S. (2018). The canonical E2Fs are required for germline development in *Arabidopsis*. Front. Plant Sci. **9**:638.

Zhang, L., Li, F., Zhang, D., Liu, X., Wang, H., Xu, Z., Chu, C., and Zhou, Y. (2017). Control of secondary cell wall patterning involves xylan deacetylation by a GDSL esterase. Nat. Plants **3**:17017.

Zhang, M.J., Zhang, X.S., and Gao, X.Q. (2020). ROS in the male-female interactions during pollination: function and regulation. Front. Plant Sci. **11**:177.